

An Actor-Critic-Identifier Control Design for Increasing Energy Efficiency of Automated Electric Vehicles

Hamed Faghihian¹, Arman Sargolzaei¹

Abstract—Electric vehicles (EVs) are increasingly deployed, yet range limitations remain a key barrier. Improving energy efficiency via advanced control is therefore essential, and emerging vehicle automation offers a promising avenue. However, many existing strategies rely on indirect surrogates because linking power consumption to control inputs is difficult. We propose a neural-network (NN) identifier that learns this mapping online and couples it with an actor–critic reinforcement learning (RL) framework to generate optimal control commands. The resulting actor–critic–identifier architecture removes dependence on explicit models relating total power, recovered energy, and inputs, while maintaining accurate speed tracking and maximizing efficiency. Update laws are derived using Lyapunov stability analysis, and performance is validated in simulation. Compared to a traditional controller, the method increases total energy recovery by 12.84%, indicating strong potential for improving EV energy efficiency.

I. Introduction

Despite the fact that electric vehicles (EVs) are bringing promising solutions for many of transportation problems, their market penetration remains constrained by range limitations [1]. However a primitive solution could be extending the battery capacity but this solution increases energy use and raises environmental, cost, and emissions concerns [2]. Therefore, the complementary solution is to improve efficiency through emerging capabilities in vehicles [3].

Automated vehicles (AVs) offer multiple potentials to increase energy efficiency through perception, signal-phase awareness, intersection coordination, or their combination [4, 5]. However, these advances are less developed for electric AVs (EAVs), where regenerative braking and different energy efficiency patterns necessitate EV-specific energy-efficient controllers development.

Recent studies in EAV included energy optimal deceleration and braking strategies with a real time extension [6], adaptive energy recovery from multi-source data [7], and automated braking to extend range [8]. However, most of these works only considered regenerative braking system, and they are not considering traffic efficiency and smoothness. Moreover, none demonstrates a controller that maximizes EAV energy efficiency within a designed driving scenario.

Energy efficiency in driving scenarios is commonly presented in the form of eco-driving which optimizes

speed along a route [9]. EV energy efficiency is also affected by battery and power electronics behavior and by mode switching, therefore consumption also depends on state dependent power flows [10]. As a result, fully coupled models that integrate the energy management system (EMS), vehicle dynamics, and powertrain are challenging to construct and remain underexplored.

Classical optimal control approaches including dynamic programming (DP), and model predictive control (MPC) propose powertrain models within EMS and vehicle dynamics to optimize speed regulation and energy use [11]. These controllers performance depends highly on accurate mappings from control to power consumption or regeneration, which are frequently uncertain and sometimes inaccessible in practice [12]; even when these maps are available, controller effectiveness is sensitive to model fidelity and computational power of the controller in realtime. To solve these issues, machine learning (ML) based method proposed which mitigate model-dependence. In particular, reinforcement learning (RL) has been used to learn energy-aware driving policies and enable adaptive control [13, 14], with applications to energy management in hybrid electric vehicles and fuel cell electric vehicles [15]. However, these studies do not target EVs and typically separates identification from control, lacking a controller that simultaneously learns the dynamics and computes an optimal policy.

Another learning based approach used for energy management in literature is Q-learning [16, 17]. Q-learning suffers from dependency to tabular schemes which bring discretizations and weak convergence guarantees [18], Deep Q-function approximators improve scalability [19, 20]. However, they still inherit discretizations problem. Another approach to avoid discretizations introduced in literature is continuous actor–critic method [21], this method is supervisory and can not handle unknown EV dynamics or enforce drive-cycle tracking while minimizing energy. We therefore utilize a NN-based, online approach that couples policy learning with system identification.

This paper proposes an actor–critic–identifier (ACI) controller that learns system behavior during acceleration and deceleration while tracking both system state and desired behavior allowing for generating an energy efficient control signal. Lyapunov-based analysis guides the update laws for actor, critic, and identifier. Our contributions are: (i) an ACI RL controller that improves EV energy efficiency with accurate drive-cycle

¹ Hamed Faghihian and Arman Sargolzaei are with the Department of Mechanical Engineering, University of South Florida, Tampa, FL 33620, USA. Emails: hfaghihian@usf.edu, a.sargolzaei@gmail.com

tracking; (ii) elimination of explicit power-consumption modeling for adaptability across EVs and conditions; (iii) designing actor, critic, and identifier update laws based on Lyapunov stability analysis.

The rest of this paper is organized as follows. In Section II, we present the EV model, cost, and optimal control formulation. In Section III, we present challenges, the ACI controller architecture, learning laws and update policies for each of NNs. In Section IV, we establish stability via Lyapunov stability analysis. In Section V, we report simulations and compare against a tuned PID baseline. In Section VI, we conclude and outline future work.

II. Problem Formulation and Objectives

The system dynamics which serve as the foundation for constructing the optimization problem is discussed in this section.

A. Dynamic model

The EV longitudinal unknown model can be represented as

$$\dot{x}(t) = F(x(t), u(t)) = g(x(t)) + h(x(t))u(t), \quad (1)$$

where $u(t) \in U \subseteq \mathbb{R}$ is the control input, which is considered here as the torque of the EV traction motor. $x(t) \in X \subseteq \mathbb{R}^2$ denotes the state vector of the system with $x_1(t) \triangleq v_v(t) - v_d(t)$, where $v_v(t)$, $v_d(t) \in \mathbb{R}$ are the vehicle longitudinal speed and the vehicle desired speed respectively, and $x_2(t) \triangleq P_{acc}(t) - P_{rb}(t)$, where $P_{acc}(t) \in \mathbb{R}$ is the power needed for acceleration, and $P_{rb}(t) \in \mathbb{R}$ is power recovered during regenerative braking. The functions $g(x(t))$, $h(x(t)) \in \mathbb{R}^2$ in (1) are considered to be second-order differentiable functions.

Assumption 1: The function $h(x)$ considered to be known and bounded such that $\|h(x)\| \leq \bar{h}$, where $\bar{h} \in \mathbb{R}^+$ is a constant value¹.

However we are assuming that $h(x)$ is known, but $g(x)$ is unknown. Therefore, the second state variable $x_2(t)$ does not show a direct relationship to the vehicle's acceleration and the relationship is unknown², which is our main challenge addressing in this paper. For simplicity of notations, the time variable t is omitted in the remainder of the paper.

B. Problem formulation

Given the dynamic model (1), and knowing that $g(x)$ is unknown, the problem statement is to design a control signal u , to minimize total energy consumption, while it keep the desired velocity. To achieve that, let's define the optimal value function $J^*(x) \in \mathbb{R}$, and the subsequent

¹We can consider $h(x)$ as a bounded function since the physical model of vehicle is bonded.

²Considering the input-power mapping as unknown is physically justified in EVs as it depends on SOC, temperature, speed/torque, efficiency maps, etc., all are time-varying, explicit models are often unavailable.

control law $u^*(x) \in \mathbb{R}$ for the system we introduced in (1) would be written as

$$\begin{cases} J^*(x) = \min_{u(\tau) \in \Pi(X)} \int_t^\infty \ell(x(s), u(x(s))) ds, \quad J^*(0) = 0 \\ u^*(x) = -\frac{1}{2}\beta^{-1}h^T(x)(\frac{\partial J^*}{\partial x}), \end{cases} \quad (2)$$

where $\Pi(X)$ is admissible control policies, $\beta \in \mathbb{R}^+$ is a constant.

To ensure speed tracking, energy efficiency, with minimum control, we designed $\ell(x, u) : X \times U \rightarrow \mathbb{R}$ as

$$\ell(x, u) = C(x) + u^T \beta u, \quad (3)$$

where the function $C(x)$ designed as

$$C(x) = q_1(v_v(t) - v_d(t))^2 + q_2 P_{accel}^2(t), \quad (4)$$

where $q_1, q_2 \in \mathbb{R}^+$ are weighting coefficients to penalizes deviation from the desired speed, and power drawn in acceleration phases. The acceleration terms, $P_{accel}(t)$ defined based on $x_2(t)$ as $P_{accel}(t) \triangleq \max(x_2(t), 0)$. This formulation allows energy consumption to be integrated into the optimization via a power parameter that can be measured experimentally or through whole-vehicle modeling.

The controller is designed by minimizing the Hamilton–Jacobi–Bellman (HJB) residual [22]. Therefor, the system Hamiltonian would be defined as

$$\mathcal{H}(x, u, J_x) \triangleq J_x F(x, u) + \ell(x, u), \quad (5)$$

where $J(x) \triangleq \int_0^\infty \ell(x(t), u(t)) dt$, and $J_x \triangleq \frac{\partial J}{\partial x} \in \mathbb{R}^{1 \times 2}$. At optimality we have

$$\mathcal{H}(x, u^*, J_x^*) = J_x^* F(x, u^*) + \ell(x, u^*) = 0, \quad (6)$$

which shows no further cost reduction under $u^*(x)$ (as in (2)). Since u^* , J^* , F are unknown, we use approximations \hat{u} , \hat{J} , \hat{F} respectively, leads to defining the HJB residual as

$$\delta_{HJB} \triangleq \hat{\mathcal{H}}(x, \hat{u}, \hat{J}_x) - \mathcal{H}(x, u^*, J_x^*) = \hat{J}_x \hat{F}(x, \hat{u}) + \ell(x, \hat{u}), \quad (7)$$

where $\hat{J}_x \triangleq \frac{\partial \hat{J}}{\partial x}$. The goal is to design a continuous policy \hat{u} that minimizes δ_{HJB} so that the realized policy tracks the optimal one in (2).

III. Method: Actor-Critic-Identifier (ACI)

A. Challenges

Designing an optimal controller for the nonlinear EV system presents three major challenges. First, the optimal value function $J^*(x)$ and control policy $u^*(x)$ exist but are unknown and must be approximated. Second, the system dynamics contain an unknown drift term $g(x)$, requiring a real-time identifier to learn and compensate for these dynamics, which is the main challenge. Third, the optimal controller must simultaneously minimize the HJB residual δ_{HJB} while ensuring stability and boundedness of all estimates under time-varying driving conditions.

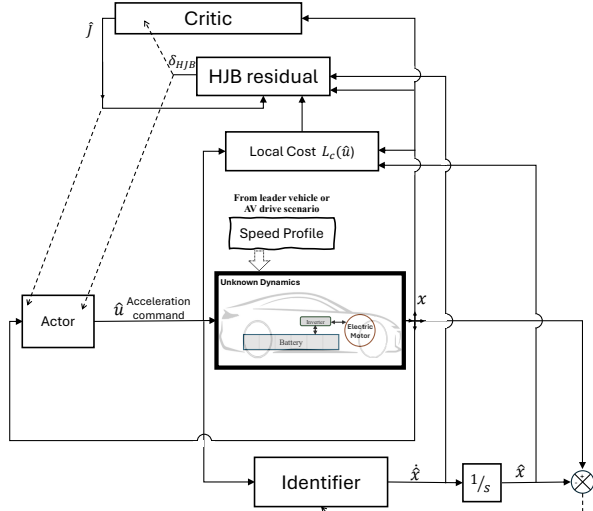


Fig. 1: The controller architecture

B. Solution Architecture

Since we need to approximate the unknown optimal value function, policy, and dynamics, we utilize three coordinated neural networks: a critic for approximation of $J^*(x)$, an actor to approximate the control policy $u^*(x)$, and an identifier to estimate the unknown part of system dynamics, $g(x)$. The three modules are coupled with the the HJB residual, δ_{HJB} , therefore, in each update the residual reducing and shift the realized policy toward the optimal one. This architecture described in Figure 1.

C. Critic Network

We approximate the value function as

$$\hat{J}(x) = \hat{w}_c^T \phi(x), \quad \phi(x) \in \mathbb{R}^N, \quad (8)$$

with basis vector $\phi(\cdot)$ and critic weights $\hat{w}_c \in \mathbb{R}^N$. Let the regressor be defined as

$$\varphi(x, \hat{x}, \hat{u}) = \phi'(x) \hat{F}(x, \hat{u}). \quad (9)$$

Based on the Lyapunov stability analysis described in Section IV, We design the critic update law with adaptation gain matrix, $\mathcal{P} \in \mathbb{R}^{N \times N}$, as

$$\dot{\hat{w}}_c = -k_{c1} \frac{\varphi}{1 + \kappa \varphi^T \mathcal{P} \varphi} \delta_{\text{HJB}} - k_{c2} (\hat{w}_a - \hat{w}_c), \quad (10)$$

$$\dot{\mathcal{P}} = -k_{c1} \mathcal{P} \frac{\varphi \varphi^T}{1 + \kappa \varphi^T \mathcal{P} \varphi} \mathcal{P}. \quad (11)$$

\mathcal{P} is initializing as $\mathcal{P}(0) = \mathcal{P}_1 I$, where $I \in \mathbb{R}^{N \times N}$ is the identity matrix and $\mathcal{P}_1 \in \mathbb{R}^+$ is a positive constant with covariance resetting to keep $0 \leq \mathcal{P}_0 I \leq \mathcal{P}(t) \leq \mathcal{P}_1 I$. Therefore, based on (11), $\dot{\mathcal{P}}(t) \leq 0$, showing $\mathcal{P}(t)$ is non-increasing over time. The covariance resetting technique employed To prevent $\mathcal{P}(t)$ to become arbitrarily small, to prevent excessively slow updates in the critic network. This would ensure stable and sufficiently responsive learning.

D. Actor Network

The actor designed to generates the control policy $\hat{u}(x)$ by approximating the optimal control $u^*(x)$. Therefore, by using the approximation method of $\hat{J}(x)$ similar to (8), we can write

$$\hat{u}(x) = -\frac{1}{2} \beta^{-1} h^T(x) \phi'(x)^T \hat{w}_a, \quad (12)$$

where $\hat{w}_a \in \mathbb{R}^N$ are actor weights. By Defining $H(x) \triangleq h(x) \beta^{-1} h^T(x)$. The actor update rule based on the Lyapunov stability analysis (Section IV) designed as

$$\begin{aligned} \dot{\hat{w}}_a = \text{proj} \left\{ -\frac{2k_{a1}}{\sqrt{1 + \varphi^T \varphi}} \left[\left(\hat{w}_c^T \phi' \frac{\partial \hat{F}(x, \hat{u})}{\partial \hat{u}} \frac{\partial \hat{u}}{\partial \hat{w}_a} \right)^T \right. \right. \\ \left. \left. + \frac{\partial \hat{u}}{\partial \hat{w}_a}^T \beta \hat{u} \right] \delta_{\text{HJB}} - k_{a2} (\hat{w}_a - \hat{w}_c) \right\}, \end{aligned} \quad (13)$$

where $\text{proj}\{\cdot\}$ enforcing boundedness.

E. Identifier Network Design

The identifier network provides approximations of system dynamic model. Based on the Lyapunov stability analysis in Section IV we designed an identifier by an NN to estimate the unknown part of the system dynamic, $g(x)$ as

$$g(x) = w_g^T \sigma(v_g^T x) + \xi_g(x), \quad (14)$$

where w_g, v_g are ideal weights and ξ_g is reconstruction error. Therefore the identifier estimates the system dynamics as

$$\dot{\hat{x}} = \hat{F}(x) = \hat{w}_g^T \hat{\sigma}_g + h(x) \hat{u} + r_t, \quad (15)$$

where $\hat{\sigma}_g \triangleq \sigma(v_g^T \hat{x})$ and r_t is a RISE feedback term defined as

$$\begin{aligned} r_t &\triangleq p_1 (\tilde{x}(t) - \tilde{x}(0)) + \nu(t), \\ \dot{\nu} &= (p_1 \alpha + \gamma) \tilde{x} + p_2 \text{sgn}(\tilde{x}), \quad \nu(0) = 0, \end{aligned} \quad (16)$$

where $\tilde{x} \triangleq x - \hat{x}$ and p_1, α, γ, p_2 are positive gains. The identifier weight updates designed using Lyapunov stability analysis provided in Section IV (with constant positive $\Upsilon_w \in \mathbb{R}^{(L_g+1) \times (L_g+1)}$ and $\Upsilon_v \in \mathbb{R}^{2 \times 2}$) are

$$\dot{\hat{w}}_g = \text{proj} \left\{ \Upsilon_w \hat{\sigma}_g' \hat{v}_g^T \dot{\hat{x}} \hat{x}^T \right\}, \quad \dot{\hat{v}}_g = \text{proj} \left\{ \Upsilon_v \dot{\hat{x}} \hat{x}^T \hat{w}_g^T \hat{\sigma}_g' \right\}. \quad (17)$$

This ACI loop yields a continuous controller \hat{u} that tracks the optimal policy without requiring the explicit power-consumption model of the vehicle.

F. HJB Residual based on NNs

The HJB residual with respect to (3), and (6)-(9) can be write as

$$\delta_{\text{HJB}} = \hat{w}_c^T \varphi + \hat{u}^T \beta \hat{u} - J_x^* F(x, u^*) - u^{*T} \beta u^*. \quad (18)$$

Substituting (12) into (18) gives

$$\begin{aligned}\delta_{\text{HJB}} = & \hat{w}_c^T \varphi + \left[-\frac{1}{2} \hat{w}_a^T \phi' h \beta^{-1} \right] \beta \left[-\frac{1}{2} \beta^{-1} h^T \phi'^T \hat{w}_a \right] \\ & - \left[-\frac{1}{2} (\xi'_v + w^T \phi') \beta^{-1} h \right] \beta \left[-\frac{1}{2} \beta^{-1} h^T (\phi'^T w + \xi'_v) \right] \\ & - [w^T \phi' + \xi'_v] F(x, u^*).\end{aligned}\quad (19)$$

With $\tilde{w}_a \triangleq w - \hat{w}_a$, $\tilde{w}_c \triangleq w - \hat{w}_c$, $\tilde{u} \triangleq u^* - \hat{u}$, and $\tilde{F}(x, \hat{u}) \triangleq F(x, \hat{u}) - \hat{F}(x, \hat{u})$, (19) simplifies to

$$\begin{aligned}\delta_{\text{HJB}} = & \hat{w}_c^T \varphi - w^T \phi' \tilde{F}(x, \hat{u}) - \xi'_v F(x, u^*) \\ & + \frac{1}{4} \tilde{w}_a^T \phi' H \phi'^T \tilde{w}_a - \frac{1}{4} \xi'_v H \xi'^T_v.\end{aligned}\quad (20)$$

IV. Stability Analysis

The actor, critic, and identifier updates are derived through Lyapunov stability analysis. To provide stability analysis we need preliminary calculations.

A. Necessary Assumptions and Calculations

Assumption 2: The ACI's NN weights, w and its approximations w_a , w_c are bounded such that $w \leq \bar{w}$, and $w_a \leq \bar{w}_a$, $w_c \leq \bar{w}_c$, $v_g \leq \bar{v}_g$, and $w_g \leq \bar{w}_g$, where \bar{w} , \bar{w}_a , and $\bar{w}_c \in \mathbb{R}^+$, \bar{v}_g , $\bar{w}_g \in \mathbb{R}^+$ are known constants.

Assumption 3: The functions $\phi(x), \xi_v(x)$ and their derivatives $\phi'(x), \xi'_v(x)$ are bounded such that

$$\begin{cases} \|\phi(x)\| \leq M_\phi \quad \text{and} \quad \|\phi'(v_g^T x)\| \leq M_{\phi'} \\ \|\xi_v(x)\| \leq M_{\xi_v} \quad \text{and} \quad \|\xi'_v(x)\| \leq M_{\xi'_v}, \end{cases}$$

where M_ϕ , $M_{\phi'}$, M_{ξ_v} , and $M_{\xi'_v}$ are positive definite constants

Assumption 4: As $N \rightarrow \infty$ the reconstruction error and its derivatives, $\xi_v(x), \xi'_v(x) \rightarrow 0$.

Assumption 5: The identifier activation $\sigma(v_g^T x)$, its derivative, and the reconstruction error $\xi_g(x)$ with its derivative are bounded; i.e., there exist $M_\sigma, M_{\sigma'}, M_\xi, M_{\xi'} > 0$ such that

$$\begin{cases} \|\sigma(v_g^T x)\| \leq M_\sigma \quad \text{and} \quad \|\sigma'(v_g^T x)\| \leq M_{\sigma'} \\ \|\xi_g(x)\| \leq M_\xi \quad \text{and} \quad \|\xi'_g(x)\| \leq M_{\xi'} \end{cases}$$

By defining $e_g \triangleq \dot{\tilde{x}} + \alpha \tilde{x}$ and Using (15), (14), and (17) we can write

$$\begin{aligned}\dot{e}_g = & \ddot{\tilde{x}} + \alpha \dot{\tilde{x}} = w_g^T \sigma'_g v_g^T \dot{x} \\ & - (\hat{w}_g^T \hat{\sigma}_g + \hat{w}_g^T \hat{\sigma}'_g \hat{v}_g^T \hat{x} + \hat{w}_g^T \hat{\sigma}'_g \hat{v}_g^T \dot{\tilde{x}}) + \dot{\xi}_g - \dot{r}_t + \alpha \dot{\tilde{x}},\end{aligned}\quad (21)$$

which can be written as

$$\dot{e}_g = T_1 + T_2 - p_1 e_g - \gamma \tilde{x} - p_2 \text{sgn}(\tilde{x}). \quad (22)$$

where

$$\begin{aligned}T_1 = & \alpha \dot{\tilde{x}} - \hat{w}_g^T \hat{\sigma}_g - \hat{w}_g^T \hat{\sigma}'_g \hat{v}_g^T \hat{x} + \frac{1}{2} w_g^T \hat{\sigma}'_g \hat{v}_g^T \dot{\tilde{x}} + \frac{1}{2} \hat{w}_g^T \hat{\sigma}'_g \hat{v}_g^T \dot{\tilde{x}}, \\ T_2 = & w_g^T \sigma'_g v_g^T \dot{x} - \frac{1}{2} w_g^T \hat{\sigma}'_g \hat{v}_g^T \dot{\tilde{x}} - \frac{1}{2} \hat{w}_g^T \hat{\sigma}'_g \hat{v}_g^T \dot{\tilde{x}} + \dot{\xi}_g, \\ T_3 = & \frac{1}{2} \tilde{w}_g^T \hat{\sigma}'_g \hat{v}_g^T \dot{\tilde{x}} + \frac{1}{2} \hat{w}_g^T \hat{\sigma}'_g \hat{v}_g^T \dot{\tilde{x}}.\end{aligned}\quad (23)$$

Remark 1: Under Assumptions 1, 2, 5, the identifier (15), and the projection bounds in (17), let $\theta \triangleq [\tilde{x}^\top \ e_g^\top]^\top$ and define

$$\begin{aligned}T_4 & \triangleq \frac{1}{2} \tilde{w}_g^\top \hat{\sigma}'_g \hat{v}_g^\top \dot{\tilde{x}} + \frac{1}{2} \hat{w}_g^\top \hat{\sigma}'_g \hat{v}_g^\top \dot{\tilde{x}}, \\ T_5 & \triangleq T_3 + T_4 = \frac{1}{2} \tilde{w}_g^\top \hat{\sigma}'_g \hat{v}_g^\top \dot{\tilde{x}} + \frac{1}{2} \hat{w}_g^\top \hat{\sigma}'_g \hat{v}_g^\top \dot{\tilde{x}}, \\ T_6 & \triangleq T_2 + T_5.\end{aligned}$$

Then there exist nondecreasing functions $\rho_1, \rho_2 : \mathbb{R}^+ \rightarrow \mathbb{R}^+$ and constants $c_1, c_2, c_3, c_4, c_5, c_6 \in \mathbb{R}^+$ such that

$$\begin{aligned}\|T_1\| & \leq \rho_1(\|\theta\|) \|\theta\|, & \|T_2\| & \leq c_1, \\ \|\dot{x}^\top T_4\| & \leq c_2 \|\dot{x}\|^2 + c_3 \|e_g\|^2, & \|T_5\| & \leq c_4, \\ \|T_6\| & \leq c_1 + c_4, & \|\dot{T}_6\| & \leq c_5 + c_6 \rho_2(\|\theta\|) \|\theta\|.\end{aligned}$$

B. Proof of Stability

Theorem 1: With the update laws (17), the identifier (15) guarantees asymptotic tracking $\|\tilde{x}(t)\|, \|\dot{\tilde{x}}(t)\| \rightarrow 0$ as $t \rightarrow \infty$ whenever

$$\begin{aligned}p_1 & > 2c_3 & p_2 & > \max\{c_1 + c_4, +c_1 + \frac{c_5}{\alpha}\}, \\ p_3 & > c_6, & \gamma & > \frac{2c_2}{\alpha}.\end{aligned}\quad (24)$$

Proof: Define $y_1 \triangleq [\tilde{x}^\top \ e_g^\top \ \sqrt{\Theta} \ \sqrt{\Omega}]^\top \in \mathbb{D} \subset \mathbb{R}^6$ and the Lyapunov candidate function as

$$V_{L_1} = \frac{1}{2} e_g^\top e_g + \frac{1}{2} \gamma \tilde{x}^\top \tilde{x} + \Theta + \Omega, \quad V_{L_1} : \mathbb{D} \rightarrow \mathbb{R} \quad (25)$$

where

$$\Omega \triangleq \frac{\alpha}{4} (\text{tr}(\tilde{w}_g^\top \Upsilon_w^{-1} \tilde{w}_g) + \text{tr}(\tilde{v}_g^\top \Upsilon_v^{-1} \tilde{v}_g)).$$

Remark 2: Let $\Theta(\theta, t) \in \mathbb{R}$ be the Filippov solution of (26) [23]:

$$\begin{aligned}\dot{\Theta} & = -e_g^T (T_2 - p_2 \text{sgn}(\tilde{x})) - \dot{\tilde{x}}^T T_5 + p_3 \rho_2(\|\theta\|) \|\theta\| \|\tilde{x}\|, \\ \Theta(0) & = p_2 \sum_{i=1}^n |\tilde{x}_i(0)| - \tilde{x}^T(0) T_6(0),\end{aligned}\quad (26)$$

Then $\Theta(t) \geq 0$ for all $t \geq 0$ if the gains satisfy $p_2 > \max\{c_1 + c_4, c_1 + c_5/\alpha\}$, and $p_3 > c_6$.

Applying conditions for Remark 2 with (25) we can find positive definite bonds, b_{11}, b_{12} on V_{L_1} , such that

$$b_{11}(y_1) \leq V_{L_1}(y_1) \leq b_{12}(y_1), \quad (27)$$

where $b_{11}(y) \triangleq \frac{1}{2} \min(1, \gamma)$ and $b_{12}(y) \triangleq \max(1, \gamma) \|y_1\|^2$.

Using Filippov's framework, a generalized Lyapunov analysis utilized. Therefore, generalized time derivative of (25) for almost all $t \in [t_0, t_f]$, can be written as

$$\dot{V}_{L_1}(y_1) \in \bigcap_{\chi \in \partial V_{L_1}(y_1)} \chi^\top K[Y](s, t), \quad (28)$$

where $Y(y_1, t) \triangleq \begin{bmatrix} \dot{e}_g^\top & \dot{\tilde{x}}^\top & \frac{1}{2} \Theta^{-\frac{1}{2}} \dot{\Theta} & \frac{1}{2} \Omega^{-\frac{1}{2}} \dot{\Omega} \end{bmatrix}^\top$, and $K[\cdot]$ is set-valued map defined as $K[J](s, t) \triangleq \bigcap_{\delta > 0} \bigcap_{R_N=0} \bar{co} J(B(s, r) - N, t)$, where \bar{co} is convex closure with $B(s, r)$ is a ball of radius r centered at s .

Since $V_{L_1}(y_1)$ is Lipschitz and regular, Filippov's operator with using the generalized Lyapunov method

for discontinuous systems [24], the right hand side of (28) can be written as

$$[e_g^T \gamma \dot{x}^T 2\Theta^{-\frac{1}{2}} 2\Omega^{-\frac{1}{2}}] K [\dot{e}_g^T \dot{x}^T \frac{1}{2}\Theta^{-\frac{1}{2}}\dot{\Theta} \frac{1}{2}\Omega^{-\frac{1}{2}}\dot{\Omega}]^T, \quad (29)$$

which we define the (29) as V_R , so we can consider $\dot{V}_{L_1}(y_1) \in V_R$. Applying (22), (26), into (29), we can rewrite V_R as

$$\begin{aligned} V_R = & e_g^T (T_1 + T_2 + T_3 - p_1 e_g - \gamma \tilde{x} - p_2 K[\text{sgn}(\tilde{x})]) \\ & + \gamma \tilde{x} (e_g - \alpha \tilde{x}) - e_g^T (T_2 - p_2 K[\text{sgn}(\tilde{x})]) \\ & - \dot{x}^T T_5 + p_3 \rho_2(\|\theta\|) \|\theta\| \|\tilde{x}\| \\ & - \frac{1}{2} \alpha \left[\text{tr} \left(\tilde{w}_g^T \Upsilon_w^{-1} \dot{w}_g \right) + \text{tr} \left(\tilde{v}_g^T \Upsilon_v^{-1} \dot{v}_g \right) \right], \end{aligned} \quad (30)$$

where $K[\text{sgn}(\tilde{x})] = \{1\}$ for $\tilde{x} > 0$, $[-1, 1]$ for $\tilde{x} = 0$, and $\{-1\}$ for $\tilde{x} < 0$. Based on this, (30) will be reduced to scalar, also by using (17), (23), and with considering Remark 1, we can rewrite and simplify it to

$$T_1 e_g - p_1 e_g^T e_g - \alpha \gamma \tilde{x}^T \tilde{x} - T_4 \dot{x}^T + p_3 \rho_2(\|\theta\|) \|\theta\| \|\tilde{x}\|. \quad (31)$$

Since the expression in (31) is continuous for $\tilde{x}(t) \neq 0$ and any discontinuities occur on a set of times of Lebesgue measure zero, by Remarks 1 and 1 we can write

$$\begin{aligned} V_R \leq & -\left(\frac{p_1}{2} - c_3\right) \|e_g\|^2 - \left(\frac{\alpha \gamma}{2} - c_2\right) \|\tilde{x}\|^2 \\ & + \left(\frac{1}{2p_1} \rho_1(\|\theta\|)^2\right) + \left(\frac{1}{2\alpha \gamma} p_2^2 [\rho_2(\|\theta\|)]^2\right) \|\theta\|^2, \end{aligned} \quad (32)$$

which can be written as

$$V_R \leq -l_1 \|\theta\|^2 + l_2((\|\theta\|)^2 \|\theta\|^2), \quad (33)$$

where $l_1 \triangleq \min\{\frac{p_1}{2} - c_3, \frac{\alpha \gamma}{2} - c_2\}$ and $l_2(\theta) \triangleq \max\{\frac{1}{2\alpha \gamma} p_2^2 [\rho_2(\|\theta\|)]^2, \frac{1}{2p_1} [\rho_1(\|\theta\|)]^2\}$. Then the right hand side of (32) can be bounded as

$$V_R \leq -l_1 \|\theta\|^2 + l_2((\|\theta\|)^2 \|\theta\|^2), \quad (34)$$

therefore, there exist p_1 and γ such that $V_R \leq -l_3 \|\theta\|^2$ where l_3 is a positive constant. This will leads to

$$\dot{V}_{L_1}(y_1) \leq -\Gamma_1(y_1), \quad \dot{V}_{L_1}(y_1) \stackrel{\text{a.e.}}{\in} \dot{R}_{L_1}(y_1), \quad (35)$$

where $\Gamma_1(y_1) \triangleq l_3 \|\theta\|^2$ is a positive, continuous, semi-definite function. applying bonds in (27), we can write

$$\dot{V}_{L_1}(y_1) \leq -\frac{\Gamma_1(y_1)}{b_{12}(y_1)} V_{L_1}. \quad (36)$$

Therefore, with choosing positive gains $\gamma > \frac{c_2}{\alpha}$ and $p_1 > c_3$ ensures, via (25), asymptotic tracking such that

$$\lim_{t \rightarrow \infty} \|\tilde{x}(t)\| = 0, \quad \lim_{t \rightarrow \infty} \|\dot{\tilde{x}}(t)\| = 0.$$

■

Theorem 2: Holding conditions of Theorem 1 with the identifier (15) and update laws (17), $x(t)$, \tilde{w}_a , and \tilde{w}_c are uniformly ultimately bounded (UUB) if and only if

$$\begin{cases} k_{a2} > \frac{k_{a1}}{4} c_8 c_9 + \frac{k_{a2} \epsilon_1}{2} + \frac{k_{c2}}{2\epsilon_2}, \\ k_{c2} + \frac{k_{c2} \epsilon_2}{2} + \frac{k_{a2}}{2\epsilon_1} > \frac{\epsilon_3}{2} + k_{a1} c_7 c_8 + k_{c1} \frac{p_1}{\kappa \mathcal{P}_0}. \end{cases} \quad (37)$$

Proof: With the Lyapunov candidate function

$$V_{L_2}(x, \tilde{w}_c, \tilde{w}_a) = J^*(x) + \frac{1}{2} \tilde{w}_c^T \tilde{w}_c + \frac{1}{2} \tilde{w}_a^T \tilde{w}_a, \quad (38)$$

and by introducing

$$\begin{aligned} b_{21}(\|y_2\|) & \triangleq \rho_{J1} + \frac{1}{2} \|\tilde{w}_c\|^2 + \frac{1}{2} \|\tilde{w}_a\|^2, \\ b_{22}(\|y_2\|) & \triangleq \rho_{J2} + \frac{1}{2} \|\tilde{w}_c\|^2 + \frac{1}{2} \|\tilde{w}_a\|^2. \end{aligned}$$

where $y_2 \triangleq [x^T, \tilde{w}_c^T, \tilde{w}_a^T]^T$, and we can show there exist $\rho_{J1}(\|x\|)$ and $\rho_{J2}(\|x\|) : [0, +\infty) \rightarrow [0, +\infty)$, as the lower and upper bounds of J^* . resulting in $b_{21}(\|y_2\|)$ and $b_{22}(\|y_2\|)$ to serve as upper and lower bonds of V_{L_2} .

With considering the control input \hat{u} , Using (1), (2) and taking time derivative of J^* , with respect to (7)

$$\dot{J}^* = -\frac{\partial J^*}{\partial x} g u^* - C(x) - u^{*T} \beta u^* + \frac{\partial J^*}{\partial x} g \hat{u}. \quad (39)$$

Therefore, the time derivative of the Lyapunov candidate function with respect to (10),and (13) would become

$$\begin{aligned} \dot{V}_{L_2} = & -\frac{\partial J^*}{\partial x} g u^* - \Omega(x) - u^{*T} \beta u^* - 2u^{*T} \beta \\ & + \tilde{w}_c^T [k_{c1} \mathcal{P} \frac{\varphi}{1 + \kappa \varphi^T \mathcal{P} \varphi} \delta_{HJB} + k_{c2} (\hat{w}_a - \hat{w}_c)] \\ & + \tilde{w}_a^T [\frac{k_{a1}}{\sqrt{1 + \varphi^T \varphi}} \phi' H \phi'^T (\hat{w}_a - \hat{w}_c) \delta_{HJB} \\ & + k_{a2} (\hat{w}_a - \hat{w}_c)]. \end{aligned} \quad (40)$$

Using (2), (5) and, as $t \rightarrow \infty$, $\hat{w}_a - \hat{w}_c = \tilde{w}_a - \tilde{w}_c$, and by defining $\Psi_1 \triangleq \varphi / \sqrt{1 + \kappa \varphi^T \mathcal{P} \varphi}$ to rewrite (40); then, invoking (20) and introducing $\Psi_2 \triangleq \frac{k_{a1}}{\sqrt{1 + \varphi^T \varphi}} \tilde{w}_a^T \phi' H \phi'^T$, the \dot{V}_{L_2} upper bounded as

$$\begin{aligned} \dot{V}_{L_2} \leq & -C(x) + \frac{1}{2} w^T \phi' H \xi_v'^T + \frac{1}{2} \xi_v' H \xi_v'^T + \frac{1}{2} w^T \phi' H \phi'^T \tilde{w}_a \\ & + \frac{1}{2} \xi_v' H \phi'^T \tilde{w}_a - \Psi_2 \tilde{w}_a \tilde{w}_c^T \varphi - \Psi_2 \tilde{w}_a w^T \phi' \tilde{F}(x, \hat{u}) \\ & + \Psi_2 \tilde{w}_c \tilde{w}_c^T \varphi + \frac{1}{4} \Psi_2 \tilde{w}_a \tilde{w}_a^T \phi' H \phi'^T - \frac{1}{4} \Psi_2 \tilde{w}_a \xi_v' H \xi_v'^T \\ & + \Psi_2 \tilde{w}_c w^T \phi' \tilde{F}(x, \hat{u}) - \Psi_2 \tilde{w}_a \phi' H \phi'^T \tilde{w}_a \xi_v' F(x, u^*) \\ & - \frac{1}{4} \Psi_2 \tilde{w}_c \tilde{w}_a^T \phi' H \phi'^T + \frac{1}{4} \Psi_2 \tilde{w}_c \xi_v' H \xi_v'^T \\ & + \Psi_2 \tilde{w}_c \xi_v' H \xi_v'^T F(x, u^*) + k_{c1} \tilde{w}_c^T \mathcal{P} \frac{\Psi_1 \Psi_1^T}{\varphi} \xi_v' H \xi_v'^T \\ & + k_{c1} \tilde{w}_c^T \mathcal{P} \frac{\Psi_1 \Psi_1^T}{4\varphi} w^T \phi' H \phi'^T - k_{c1} \tilde{w}_c^T \mathcal{P} \frac{\Psi_1 \Psi_1^T}{4\varphi} \xi_v' H \xi_v'^T \\ & - k_{c1} \tilde{w}_c^T \mathcal{P} \frac{\Psi_1 \Psi_1^T}{\varphi} w^T \phi' \tilde{F}(x, \hat{u}) - k_{c1} \tilde{w}_c^T \mathcal{P} \frac{\Psi_1 \Psi_1^T}{\varphi} \xi_v' F(x, u^*) \\ & + k_{a2} \tilde{w}_a^T \tilde{w}_c - k_{a2} \tilde{w}_a^T \tilde{w}_a + k_{c2} \tilde{w}_c^T \tilde{w}_a - k_{c2} \tilde{w}_c^T \tilde{w}_c. \end{aligned} \quad (41)$$

Remark 3: Under Assumptions 1-3, there exists $c_7, c_8, c_{10}, c_9 \in \mathbb{R}^+$ such that

$$\begin{aligned} \|\tilde{w}_a\| & \leq c_7, \quad \|\phi' H \phi'^T\| \leq c_8, \quad \|\xi_v' H \xi_v'^T\| \leq c_9, \\ \left\| \frac{1}{2} w^T \phi' H \xi_v'^T + \frac{1}{2} \xi_v' H \xi_v'^T + \frac{1}{2} w^T \phi' H \phi'^T \tilde{w}_a \right. \\ & \left. + \frac{1}{2} \xi_v' H \phi'^T \tilde{w}_a \right\| \leq c_{10}. \end{aligned}$$

Remark 4: Holding Theorem 1 there exist $c_{11}, c_{12} \in \mathbb{R}^+$ such that $\|w^T \phi' \tilde{F}(x, \hat{u})\| \leq c_{11}$, $\|\xi_v' F(x, u^*)\| \leq c_{12}$

Using (41) together with Remarks 3, 4, the bound $|\Psi_1 \Psi_1^T| \leq 1/(\kappa \mathcal{P}_0)$, and Young's inequality with $\epsilon_1, \epsilon_2 \in \mathbb{R}$ as positive constants, we obtain

$$\begin{aligned} \dot{V}_{L_2} &\leq -C(x) + c_{10} - (k_{a2} - \frac{k_{a1}}{4}c_8c_9 + \frac{k_{a2}\epsilon_1}{2} + \frac{k_{c2}}{2\epsilon_2})\|\tilde{w}_a\|^2 \\ &\quad - (k_{c2} - k_{a1}c_7c_8 - k_{c1}\frac{\mathcal{P}_1}{\kappa \mathcal{P}_0} + \frac{k_{a2}}{2\epsilon_1} + \frac{k_{c2}\epsilon_2}{2})\|\tilde{w}_c\|^2 \\ &\quad + [k_{a1}c_7c_8(c_7 + c_{11} + c_7c_8 + c_9 + c_{12}) + \\ &\quad k_{c1}\frac{\mathcal{P}_1}{2\sqrt{\kappa \mathcal{P}_0}}(c_{11} + c_7c_8 + \frac{c_9}{4} + c_{12})]\|\tilde{w}_c\| \\ &\quad + k_{a1}c_7^2c_8c_{11} + c_7^2c_8 + c_7c_{12}. \end{aligned} \quad (42)$$

With more simplification, and applying Young's inequality Applying Young's inequality along with bonds in(37) we can write

$$\begin{aligned} \dot{V}_{L_2} &\leq -C(x) - [(k_{a2} - \frac{k_{a1}}{4}c_8c_9 + \frac{k_{a2}\epsilon_1}{2} + \frac{k_{c2}}{2\epsilon_2})]\|\tilde{w}_a\|^2 \\ &\quad - \left[(k_{c2} - k_{a1}c_7c_8 - k_{c1}\frac{\mathcal{P}_1}{\kappa \mathcal{P}_0} + \frac{k_{a2}}{2\epsilon_1} + \frac{k_{c2}\epsilon_2}{2}) - \frac{\epsilon_3}{2} \right]\|\tilde{w}_c\|^2 \\ &\quad + \frac{1}{2\epsilon_3} \left[k_{a1}c_7c_8(c_7 + c_{11} + c_7c_8 + c_9 + c_{12}) + \right. \\ &\quad \left. k_{c1}\frac{\mathcal{P}_1}{2\sqrt{\kappa \mathcal{P}_0}}(c_{11} + c_7c_8 + \frac{c_9}{4} + c_{12}) \right]^2 \\ &\quad + (k_{a1}c_7c_8)c_7c_{11} + c_7^2c_8 + c_7c_{12} + c_{10}. \end{aligned} \quad (43)$$

where $\epsilon_3 \in \mathbb{R}$ is a positive constant. Since $C(x)$ is positive definite, there exists a strictly increasing function $\Gamma_2 : [0, \infty) \rightarrow [0, \infty)$ such that

$$\begin{aligned} \Gamma_2(\|y_2\|) &\leq C(x) + \left(k_{a2} - \frac{k_{a1}}{4}c_8c_9 + \frac{k_{a2}\epsilon_1}{2} + \frac{k_{c2}}{2\epsilon_2} \right)\|\tilde{w}_a\|^2 \\ &\quad + \left(k_{c2} - k_{a1}c_7c_8 - k_{c1}\frac{\mathcal{P}_1}{\kappa \mathcal{P}_0} + \frac{k_{a2}}{2\epsilon_1} + \frac{k_{c2}\epsilon_2}{2} - \frac{\epsilon_3}{2} \right)\|\tilde{w}_c\|^2. \end{aligned}$$

Therefore, from (43), we can write,

$$\begin{aligned} \dot{V}_{L_2} &\leq -\Gamma_2(\|y_2\|) + k_{a1}c_7^2c_8c_{11} + c_7^2c_8 + c_7c_{12} + c_{10} \\ &\quad + \frac{1}{2\epsilon_3} \left[k_{a1}c_7c_8(c_7 + c_{11} + c_7c_8 + c_9 + c_{12}) + \right. \\ &\quad \left. k_{c1}\frac{\mathcal{P}_1}{2\sqrt{\kappa \mathcal{P}_0}}(c_{11} + c_7c_8 + \frac{c_9}{4} + c_{12}) \right]^2. \end{aligned} \quad (44)$$

With considering bonds on the Lyapunov candidate function, we can write

$$\begin{aligned} \dot{V}_{L_2} &\leq -\frac{\Gamma_2(\|y_2\|)}{b_{22}(\|y_2\|)}V_{L_2} + k_{a1}c_7^2c_8c_{11} + c_7^2c_8 + c_7c_{12} + c_{10} \\ &\quad + \frac{1}{2\epsilon_3} \left[k_{a1}c_7c_8(c_7 + c_{11} + c_7c_8 + c_9 + c_{12}) + \right. \\ &\quad \left. k_{c1}\frac{\mathcal{P}_1}{2\sqrt{\kappa \mathcal{P}_0}}(c_{11} + c_7c_8 + \frac{c_9}{4} + c_{12}) \right]^2. \end{aligned} \quad (45)$$

The inequality in (45) ensure semi-global UUB of y_2 . Moreover, by Assumption 4, increasing the NN size will yields $\xi'_v \rightarrow 0$; therefore, as $t \rightarrow \infty$, the actor-critic weight errors satisfy $\tilde{w}_a \rightarrow 0$ and $\tilde{w}_c \rightarrow 0$. \blacksquare

TABLE I: NN structures and controller gains

Block	Item	Definition / Value
Identifier	Activation, L_g	$\sigma_g(z) = \frac{2}{1 + \exp(-v_g^T \hat{x})} - 1, 5$
	p_1, p_2	80, 0.2
	α, γ	300, 5
Actor–Critic	Υ_w, Υ_v	$0.1 I_{6 \times 6}, 0.1 I_{2 \times 2}$
	$\phi(x), N$	$\phi(x) = [x_1^2 \ x_1x_2 \ x_2^2]^T, 3$
	k_{a1}, k_{a2}	10, 50
	k_{c1}, k_{c2}	11, 30
	κ	0.005

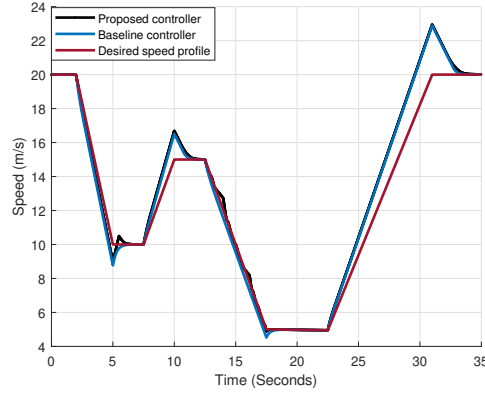


Fig. 2: Desired profile versus trajectories under the proposed ACI controller and the baseline controller.

V. Results

To evaluate the ACI controller on an EV with unknown dynamics, we embed a realistic model of powertrain–dynamics plant from [25] into the loop as described in Figure. 1 and the plant is treated as a black box. The controller identify the unknown system dynamics online, track the desired speed, and improve energy efficiency. We assume the function $h(x)$ is known and constant, chosen as $h_1((v_v - v_d), P_{ntp}) = 0$, $h_2((v_v - v_d), P_{ntp}) = 1$. The NN structures and parameter values are summarized in Table I.

To evaluate the proposed controller, we considered a representative drivecycle that can be generated by a motion planner system for AVs or induced by traffic. The EV supposed to track the drivecycle profile. As a baseline, we implemented and tuned a PID controller for the same objective, and we compared performance of our proposed controller against the PID controller performance. This comparison shown in Figure 2.

Since the controller is designed to drive the system states to zero, we showed the controller states trajectories in Figure 3 and 4 respectively. Also in order to be able to measure how much the total net traction power³ The Figure 4 also shows each controller power took from the

³The net traction power defined as the power used for longitudinal acceleration/deceleration; aerodynamic, rolling-resistance, and friction losses are excluded.

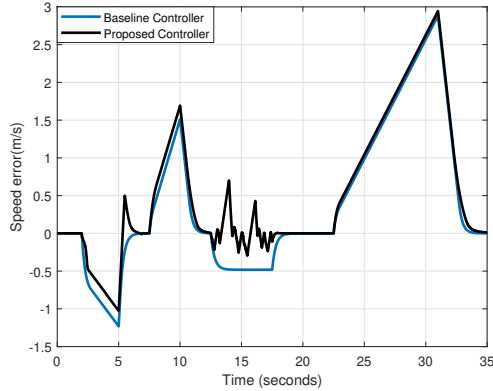


Fig. 3: Speed-tracking error over the drivecycle for the proposed ACI controller and the baseline controller.

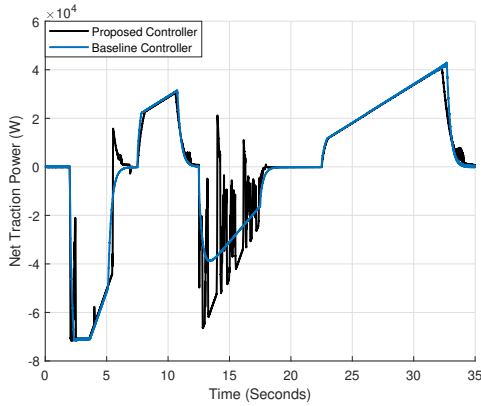


Fig. 4: Net traction power over the drive cycle for the proposed ACI controller and the baseline controller.

EV battery. Note that the positive values of power means that the power used from battery and the negative power showing the power recharging back to the EV battery due to the RBS.

The net traction energy over the drive cycle is obtained by integrating the net traction power signal. We can perform this measurement to indicate how much energy consumed or recaptured under same drivecycle with different controllers. The baseline PID consumes almost 13.835 kJ, whereas the proposed ACI controller consumes almost 7.99 kJ, which is a 42% reduction. Because the initial and final speeds are equal, this gap primarily reflects drivetrain conversion losses, which the proposed ACI controller reduces those losses. The comparison of this effect shown in Table II.

TABLE II: Comparison of total energy consumption between the proposed and baseline controllers

Controller	Energy consumed
Proposed ACI controller	7.99 KJ
Baseline PID controller	13.835 KJ

VI. Conclusion

This study showed a design procedure for an ACI controller aiming at maximizing energy efficiency while maintaining accurate drive-cycle tracking for an EV with unknown dynamics. For the design purpose a Lyapunov/Filippov analysis utilized.

Simulations on a realistic integrated EV powertrain-dynamics model show that the proposed controller achieves lower tracking error than a tuned PID baseline and reduces net traction energy over the drivecycle by a 42%. These results indicate that energy-aware optimal control can be realized without an explicit power-consumption model, relying instead on online identification and policy learning.

Future works will focus on hardware-in-the-loop and on-road experiments, and integration with connected-vehicle information. Another possible future work would be developing a two-mode controller design that treats coasting/regenerative braking separately from traction/acceleration, we expect this separation would increase energy recovery and overall efficiency.

References

- [1] H. Faghidian and A. Sargolzaei, "Energy efficiency of connected autonomous vehicles: A review," *Electronics*, vol. 12, no. 19, p. 4086, 2023.
- [2] C. R. Hung, S. Völler, M. Agez, G. Majeau-Bettez, and A. H. Strømmen, "Regionalized climate footprints of battery electric vehicles in europe," *Journal of Cleaner Production*, vol. 322, p. 129052, 2021.
- [3] H. Faghidian, J. Holland, and A. Sargolzaei, "Introduction to autonomous vehicles," in *Handbook of Power Electronics in Autonomous and Electric Vehicles*, pp. 1–16, Elsevier, 2024.
- [4] S. B. Al Islam, H. A. Aziz, H. Wang, and S. E. Young, "Minimizing energy consumption from connected signalized intersections by reinforcement learning," in *2018 21st International Conference on Intelligent Transportation Systems (ITSC)*, pp. 1870–1875, IEEE, 2018.
- [5] H. Chen, F. Wu, and T. Z. Qiu, "Achieving energy-efficient and travel time-optimized trajectory and signal control for caevs," *IEEE Transactions on Intelligent Transportation Systems*, 2024.
- [6] D. Kim, J. S. Eo, and K.-K. K. Kim, "Parameterized energy-optimal regenerative braking strategy for connected and autonomous electrified vehicles: A real-time dynamic programming approach," *IEEE Access*, vol. 9, pp. 103167–103183, 2021.
- [7] Y. Shang, C. Ma, K. Yang, and D. Tan, "Regenerative braking control strategy based on multi-source information fusion under environment perception," *International Journal of Automotive Technology*, vol. 23, no. 3, pp. 805–815, 2022.
- [8] H. Faghidian, J. Holland, and A. Sargolzaei, "Chapter 1 - introduction to autonomous vehicles," in *Handbook of Power Electronics in Autonomous and Electric Vehicles* (M. H. Rashid, ed.), pp. 1–16, Academic Press, 2024.
- [9] Y. H. Mahmoud, N. E. Brown, F. Motallebiaragh, M. Koelling, R. Meyer, Z. D. Asher, A. Dontchev, and I. Kolmanovsky, "Autonomous eco-driving with traffic light and lead vehicle constraints: An application of best constrained interpolation," *IFAC-PapersOnLine*, vol. 54, no. 10, pp. 45–50, 2021.
- [10] M. Yao, B. Zhu, and N. Zhang, "Adaptive real-time optimal control for energy management strategy of extended range electric vehicle," *Energy Conversion and Management*, vol. 234, p. 113874, 2021.

- [11] H. M. Y. Naeem, A. I. Bhatti, Y. A. Butt, Q. Ahmed, and X. Bai, "Energy efficient solution for connected electric vehicle and battery health management using eco-driving under uncertain environmental conditions," *IEEE Transactions on Intelligent Vehicles*, 2024.
- [12] J. Jeong, B. Ghaddar, N. Zufferey, and J. Nathwani, "Adaptive robust electric vehicle routing under energy consumption uncertainty," *Transportation Research Part C: Emerging Technologies*, vol. 160, p. 104529, 2024.
- [13] D. Isele, R. Rahimi, A. Cosgun, K. Subramanian, and K. Fujimura, "Navigating occluded intersections with autonomous vehicles using deep reinforcement learning," in *2018 IEEE international conference on robotics and automation (ICRA)*, pp. 2034–2039, IEEE, 2018.
- [14] J. Chen, Z. Xue, and D. Fan, "Deep reinforcement learning based left-turn connected and automated vehicle control at signalized intersection in vehicle-to-infrastructure environment," *Information*, vol. 11, no. 2, p. 77, 2020.
- [15] H. Lee and S. W. Cha, "Energy management strategy of fuel cell electric vehicles using model-based reinforcement learning with data-driven model update," *IEEE Access*, vol. 9, pp. 59244–59254, 2021.
- [16] R. Xiong, Y. Duan, J. Cao, and Q. Yu, "Battery and ultracapacitor in-the-loop approach to validate a real-time power management method for an all-climate electric vehicle," *Applied energy*, vol. 217, pp. 153–165, 2018.
- [17] B. E. Nyong-Bassey, D. Giaouris, C. Patsios, S. Papadopoulou, A. I. Papadopoulos, S. Walker, S. Voutetakis, P. Seferlis, and S. Gadoue, "Reinforcement learning based adaptive power pinch analysis for energy management of stand-alone hybrid energy storage systems considering uncertainty," *Energy*, vol. 193, p. 116622, 2020.
- [18] X. Hu, T. Liu, X. Qi, and M. Barth, "Reinforcement learning for hybrid and plug-in hybrid electric vehicle energy management: Recent advances and prospects," *IEEE Industrial Electronics Magazine*, vol. 13, no. 3, pp. 16–25, 2019.
- [19] G. Du, Y. Zou, X. Zhang, L. Guo, and N. Guo, "Heuristic energy management strategy of hybrid electric vehicle based on deep reinforcement learning with accelerated gradient optimization," *IEEE Transactions on Transportation Electrification*, vol. 7, no. 4, pp. 2194–2208, 2021.
- [20] H. He, Y. Wang, J. Li, J. Dou, R. Lian, and Y. Li, "An improved energy management strategy for hybrid electric vehicles integrating multistates of vehicle-traffic information," *IEEE Transactions on Transportation Electrification*, vol. 7, no. 3, pp. 1161–1172, 2021.
- [21] T. Haarnoja, A. Zhou, P. Abbeel, and S. Levine, "Soft actor-critic: Off-policy maximum entropy deep reinforcement learning with a stochastic actor," in *International conference on machine learning*, pp. 1861–1870, PMLR, 2018.
- [22] R. Kamalapurkar, P. Walters, J. Rosenfeld, and W. Dixon, *Reinforcement learning for optimal feedback control*. Springer, 2018.
- [23] A. F. Filippov, *Differential equations with discontinuous righthand sides: control systems*, vol. 18. Springer Science & Business Media, 2013.
- [24] Z. Guo and L. Huang, "Generalized lyapunov method for discontinuous systems," *Nonlinear Analysis: Theory, Methods & Applications*, vol. 71, no. 7-8, pp. 3083–3092, 2009.
- [25] H. Faghilian and A. Sargolzei, "A novel energy-efficient automated regenerative braking system," *Applied Energy*, 2025.